Persistent positive and transient absolute negative photoconductivity observed in diamond photodetectors

Meiyong Liao,[1,*] Yasuo Koide,[1] Jose Alvarez,[2] Masataka Imura,[1] and Jean-Paul Kleider[2]
[1]*Sensor Materials Center, National Institute for Materials Science (NIMS) 1-1 Namiki, Tsukuba, Ibaraki 305-0044, Japan*
[2]*Laboratoire de Génie Electrique de Paris (UMR 8507 CNRS), Ecole Supérieure d'Electricité, Universités Paris VI et Paris XI, 11 rue Joliot-Curie Plateau de Moulon, F-91192 Gif-sur-Yvette Cedex, France*
(Received 2 May 2008; revised manuscript received 10 June 2008; published 21 July 2008)

Persistent photoconductivity and optical quenching phenomena in boron-doped homoepitaxial diamond thin films grown on type Ib (100) substrates were investigated. Boron doping induced positive persistent photoconductivity (PPPC) and photocurrent gain upon the illumination of deep ultraviolet (DUV) light. A deep defect with a thermal energy of around 1.37 eV was deduced from the results of thermally stimulated current measurements. An optical quenching experiment revealed a threshold photon energy of around 2 eV. The difference between the thermal and optical energies of the deep defect suggests a large lattice relaxation. An absolute transient negative photocurrent (TNPC) was observed for zero or weak electric fields with DUV light illumination after optically quenching the PPPC. The absolute TNPC was due to transient electron filling of the charged nitrogen in the substrate. The combination of the nitrogen in the substrate and the boron-related defects in the epilayer was apparently responsible for the PPPC and TNPC effects. Therefore, the overall photoresponse properties of a thin epilayer deposited on a type Ib diamond substrate can be tailored by adjusting the concentration of nitrogen in the substrate and of boron in the epilayer.

DOI: 10.1103/PhysRevB.78.045112 PACS number(s): 85.60.Gz, 73.50.Pz, 73.23.Ra

I. INTRODUCTION

Wide-band-gap diamond is of great interest for solar-blind deep ultraviolet (DUV) and radiation detectors. The performance of diamond photodetectors is limited by persistent photoconductivity (PPC) and sub-band-gap photoresponse. PPC is a metastable effect that originates from macroscopic or microscopic barriers and appears quite often in many types of semiconductors.[1–3] Various defects such as grain boundaries and non-diamond phases are mostly responsible for the PPC effect and for visible light photoresponse in polycrystalline diamonds.[4–6] The use of homoepitaxial single-crystalline diamond films has been pursued to avoid these negative effects.[7–10] However, recent work on homoepitaxial diamond layers still revealed the appearance of PPC,[8,11] and PPC is often related to a photocurrent gain. It is thus essential to clarify the mechanism of PPC and gain to enable the development of high-speed diamond DUV detectors with high sensitivity.

Type Ib single crystalline diamond with a high nitrogen content is the most widely used substrate for homoepitaxial growth. The nitrogen acts as a donor and has a thermal activation energy of 1.7 eV below the conduction band.[12] Geis *et al.*[13] postulated that ionization of the nitrogen interacts with the diamond epilayer, which modulates the charge distribution in the substrate and epilayer, leading to optical switching behavior. Since the properties of a photodetector based on a thin homoepitaxial layer are affected by the substrate nitrogen, the role of nitrogen in PPC needs to be clarified. In the present work, we show direct evidence of interaction between the epilayer and the substrate by observing the transient photoconductivity.

Boron is, as far as it is known, the prevalent acceptor dopant in diamond, and it produces a complex electronic structure. One prominent feature of this structure is that it induces *p*-type conductivity with ionization energy of 0.37 eV. There are also other energy levels associated with boron impurity. Nebel *et al.*[14] suggested the existence of long-life excited states at 0.200, 0.240, and 0.266 eV above the 1-s ground state in highly boron-doped diamond, which interact with an unidentified defect at 3.36 eV. A deep level at 1.3 eV above the valence band was detected by Muret *et al.*[15] Ruan *et al.*[16,17] claimed that the optical transition at 2.3 eV strongly depends on the boron concentration. Lawson *et al.*[18] observed a luminescence band at 4.6 eV, a region rich in boron and deficient in nitrogen. However, the effect of boron on the photoresponse properties of diamond photodetectors with DUV light illumination remains unclear.

The aim of our work reported here was to clarify the photocurrent decay mechanism and gain of photodetectors fabricated on boron-doped diamond thin epilayers deposited on type Ib diamond substrates. We investigated the effect of boron doping on the photoresponse behavior by conducting experiments to measure the thermally stimulated current (TSC), PPC decay, and optical quenching.

II. EXPERIMENTS

We grew homoepitaxial diamond layers on high-pressure high-temperature synthetic Ib (100) diamond substrates using microwave plasma-enhanced chemical vapor deposition. The source gases were CH_4 and H_2. To grow high-quality epilayers, we used a low ratio (0.08%) of CH_4 (0.4 ppm) to H_2 (500 ppm), which resulted in a low growth rate (around 50 nm/h). The diamond epilayers were either intentionally or unintentionally boron doped. Prior to film growth, the substrates were sequentially boiled in HNO_3 solution containing $NaClO_3$ for 3 h, boiled in a mixture solution of HF and HNO_3 for 1 h, and cleaned in flowing deionized water for 30 min. Boron doping was done using trimethylboron

TABLE I. Devices used

Device	Sample	Structure
A	Boron-doped epilayer/Ib	SPD
B	Unintentionally doped epilayer/Ib	SPD
C	Unintentionally doped epilayer/Ib	MSM
D	Ib substrate	MSM
E	Unintentionally doped epilayer/IIa	MSM

$[B(CH_3)_3, TMB]$ gas with a flow rate of 3 ppm. The substrate temperature was 900–950 °C. The epilayer thickness was around 500 nm. The boron concentrations of the doped and undoped epilayers were around 10^{16} and below 10^{15} cm^{-3}, respectively. Both Schottky photodiode (SPD) and metal-semiconductor-metal (MSM) photoconductors with interdigitated fingers were fabricated. Prior to fabricating the devices, the epilayers were dipped in a boiling acid solution of H_2SO_4 and HNO_3 for 1 h to oxidize them. The SPD was constructed from a Ti/WC ohmic contact and a semitransparent WC or HfN Schottky contact.[8,19] The diameter of the Schottky contact was 420 ϵm, and the interspacing between the Schottky and ohmic contacts was 10 μm. The MSM planar photoconductors were fabricated on an undoped epilayer.[11] The MSM device was ohmic metallized by annealing the Ti/WC contact at 600 °C for 1 h in argon ambient. Five types of devices were fabricated and tested, as listed in Table I.

The electrical and spectral measurements were carried out in a vacuum chamber at a pressure of 0.1 Pa. The spectral response was measured using a 500-W Ushio xenon lamp and an Acton monochromator with order sorting filters. White light (WL) was obtained by setting the wavelength to zero in a spectrometer without a UV component. The transient photoconductivity for the SPDs was measured by illuminating 220-nm light (DUV) at forward biases. The following experiments were performed to examine the PPC behavior: (i) photocurrent decay for various devices under dark conditions, (ii) photocurrent decay at different temperatures for the boron-doped device, (iii) PPC quenching using WL illumination at various biases, and (iv) spectrally dependent PPC quenching. The transient photoresponse on the DUV light illumination after optically quenching the PPC effect was also measured. The TSC (Ref. 20) and PPC decay experiments for defect identification were performed at Laboratoire de Génie Électrique de Paris (LGEP), Centre National de la Recherche Scientifique (CNRS) at 300 to 600 K. For the experiments at LGEP, deuterium and halogen lamps were used for the DUV and WL illumination, respectively.

III. RESULTS

The dark current-voltage (*I-V*) characteristics for device A are shown in Fig. 1, and the device configuration is illustrated in the inset. The current was around 10^{-7} A at a forward bias, V_F, of −5 V and lower than 10^{-13} A at a reverse bias, V_R, of up to 30 V. The Schottky barrier height and the ideality factor of the Schottky diode were around 1.5 eV and 2, respectively. Note that the phenomena we observed at the forward biases did not depend on the ideality of the diode. For the other devices, little dark current ($\leq 10^{-13}$ A) was detected at ±5 V.

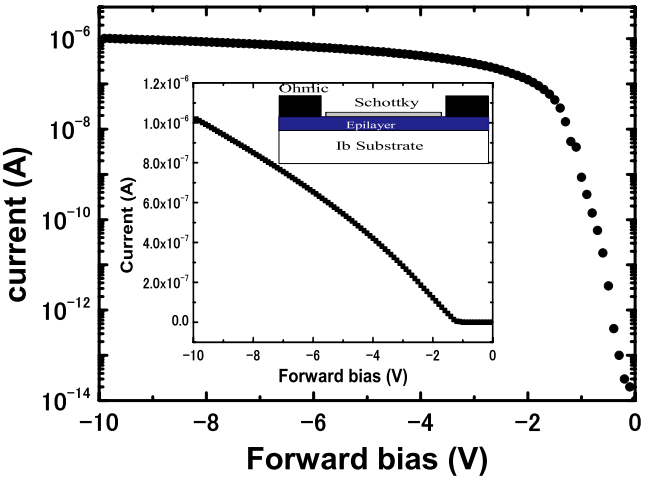

FIG. 1. (Color online). Dark *I-V* characteristics for device A. Inset shows device configuration.

A. Positive persistent photoconductivity

Figure 2(a) shows the time response of SPD device A with a boron concentration, N_B, of 10^{16} cm^{-3} at V_F=−5 V with DUV light illumination. Long-time photocurrent decay was observed following the illumination. We term this decay

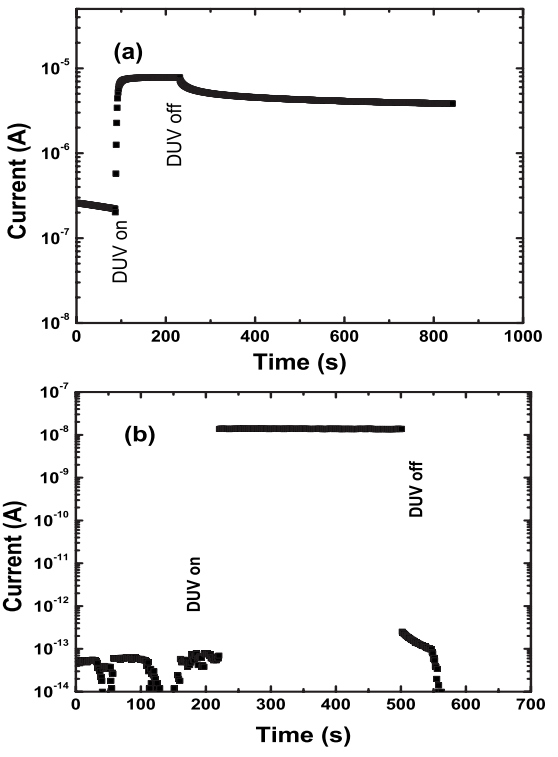

FIG. 2. Time response of devices (a) A and (b) B with 220-nm-light illumination at a forward bias of V_F=−5 V.

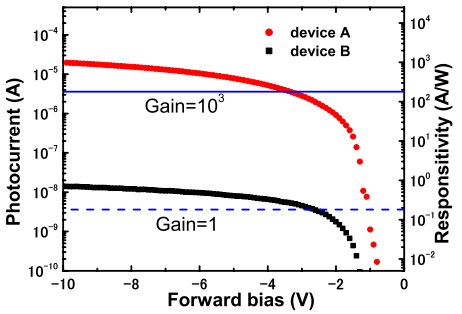

FIG. 3. (Color online). *I-V* characteristics with 220-nm-light illumination for devices A and B (right-side axis shows corresponding responsivity).

positive PPC (PPPC). Figure 2(b) shows the time response of SPD device B with a low N_B concentration ($<10^{15}$ cm^{-3}) at $V_F=-5$ V. Note that almost no PPPC appeared and that the photocurrent decreased by five orders of magnitude within 1 s after the DUV light was switched off.

The *I-V* characteristics of devices A and B with DUV light illumination in forward-bias mode are plotted in Fig. 3. The right axis shows the corresponding responsivity. The photocurrent of device A was much larger than that of device B. The photocurrent gain was more than 10^3 for device A and around 5 for device B at $V_F=-10$ V for an assumed quantum efficiency of unity.[21] Since the Schottky barrier height at the interface between WC and diamond is around 1.5 eV, the devices behaves like a photoconductor at $V_F<-2$ V. These results show that the PPPC and gain increased with the boron concentration.

B. Determination of thermal energy of deep defect

PPPC is usually related to the capture and emission processes of carriers through deep defects. The thermal activation energy of the deep defect in the boron-doped diamond sample was determined by the TSC method at a bias of –2 V. The TSC curves (Fig. 4) were recorded after a steady PPPC state was reached under DUV light illumination by a deuterium lamp. The curve shown in Fig. 4(a) indicates that there were multiple levels in the sample. To determine the thermal activation energy of the deep defect, we used WL illumination after the DUV light illumination. This process is effective to separate the TSC signal, which leads to a dominant peak with a maximum T_m at around 470 K in the TSC curve, as illustrated in Fig. 4(b). By plotting $\ln(\gamma/T_m^2)$ vs $1/T_m$ for various heating rates γ,[22] we obtained an energy level of around 1.37 eV for the peak, as shown in Fig. 5.

The thermal energy of the deep defect was also measured by the photocurrent decays at different temperatures from 300 to 500 K. Figure 6 displays the normalized PPPC at $V_F=-2$ V for three typical temperatures. The PPPC remained strong even at 420 K but decayed rapidly at 500 K. We fit the experimental PPPC decay curves with a stretched-exponential function:[23]

$$I(t) = I_0 \exp[-(t/\tau)^{\beta}](0 < \beta < 1), \quad (1)$$

where β is the decay exponent, τ is the decay time constant at a certain temperature, $I(t)$ is the current at time t, and I_0 is

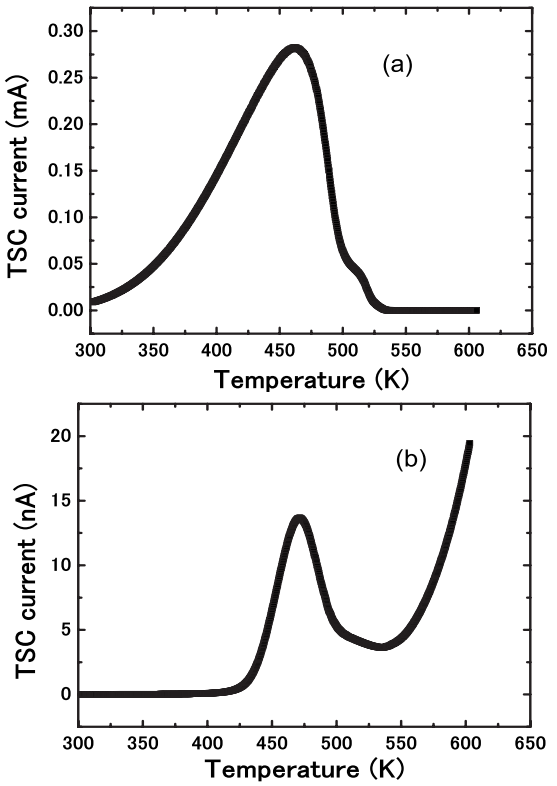

FIG. 4. TSC spectra of device A for a bias of –2 V at a heating speed of 0.25 K/s. (a) after DUV light illumination to a steady state, and (b) after DUV light followed by WL illumination.

the built-up photocurrent immediately after the DUV light was switched off. The decay curves are well fitted by Eq. (1) when β is set to 0.7. The extracted τ was plotted as a function of the temperature, as shown in Fig. 7. The decay time related to the thermal-activated recombination can be described as[23]

$$\tau \propto \exp(E_a/kT), \quad (2)$$

where E_a represents the thermal activation energy of the carrier capture barrier. The fitting of Fig. 7 using Eq. (2) results in an activation energy of $E_a=1.5$ eV, which is close to that obtained with the TSC technique. The same value was ob-

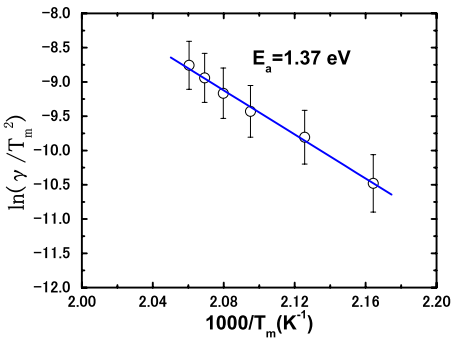

FIG. 5. (Color online). Arrhenius plot of the TSC peak after WL illumination. The slope gives a thermal activation energy of E_t =1.37 eV.

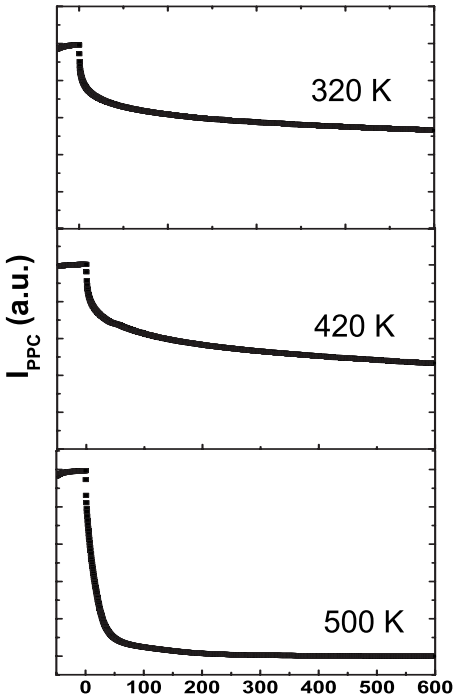

FIG. 6. Normalized PPPC decay dynamics at different temperatures for a bias of −2 V.

tained when the bias was set to V_F=−5 V. The energies determined by the TSC and PPPC decay methods should originate from the same deep defect since the fittings were made in similar temperature regimes.

C. Optical quenching of positive persistent photoconductivity

We investigated the effect of the WL illumination at various biases on the PPPC at room temperature. Figure 8(a) shows the photocurrent decay for device A at a constant bias of V_F=−5 V, following DUV light illumination. During the decay in dark conditions, the turning on and off of the bias had no effect on the decay rate. When the device was illuminated with WL, the current dropped markedly and remained at a lower level. It dropped further when the WL illumination was switched off. The PPPC was quenched by

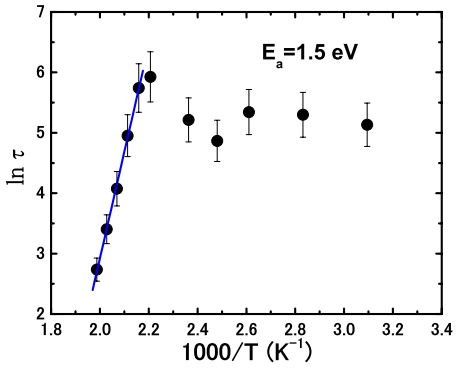

FIG. 7. (Color online). Dependence of the time constants in the PPPC on measurement temperature. The slope at high temperatures gives a thermal barrier of 1.5 eV.

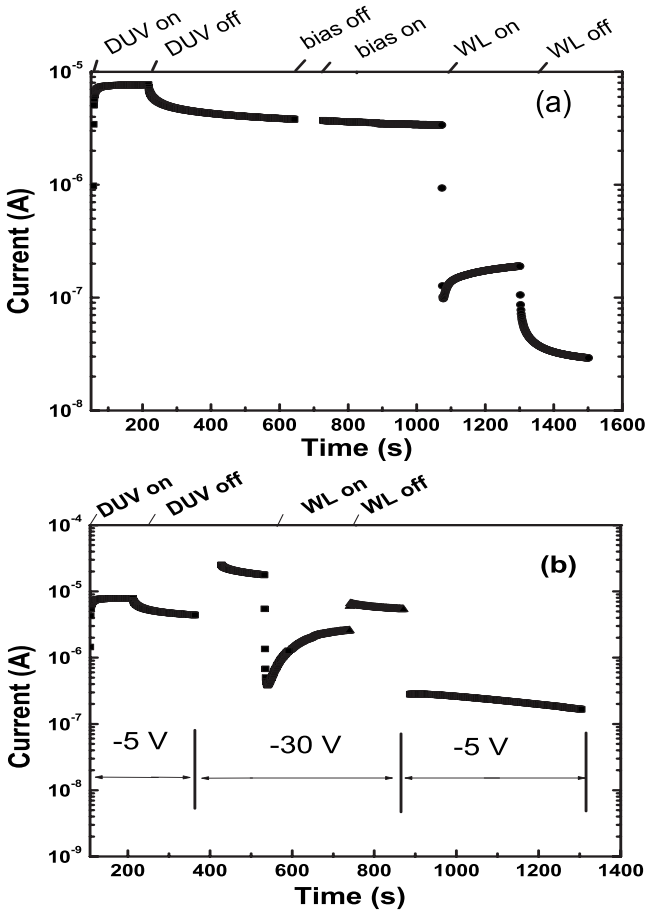

FIG. 8. Evolution of the PPPC at V_F=−5 V with time before and after the illumination of WL at (a) V_F=−5 V and (b) V_F=−30 V, where DUV represents the 220 nm light.

the WL illumination. On the other hand, the WL illumination generated a portion of photocurrent without PPPC. After quenching, the device was illuminated by the DUV light again to reach the PPPC state. Figure 8(b) shows the time decay of the PPPC at V_F=−5 V after WL illumination at V_F=−30 V. The increase in the forward bias during quenching did not speed up the current decay either in dark conditions or under WL illumination.

We examined the PPPC quenching by changing the bias polarity to reverse-bias mode during WL illumination, as illustrated in Fig. 9. The device was initially illuminated with DUV light to obtain the PPPC state at V_F=−5 V. During current decay in the dark, the bias polarity was switched to the reverse mode with V_R=10 or 30 V. The decrease in the current was simply due to the photodiode operating in reverse-bias mode. When the device was illuminated with WL, a quick rise in the current was observed. After WL illumination for hundreds of seconds, the device was then kept in the dark at V_R=10 or 30 V for hundreds of seconds. Finally, the bias was again switched to a forward bias of −5 V. The PPPC quenching at V_R=10 V shown in Fig. 9(a) is similar to that shown in Fig. 8(a). The interesting finding here is that the PPPC was completely quenched at V_R=30 V, as shown in Fig. 9(b). This quenching at reverse bias caused the photodiode to be insulating at all the investigated forward biases.

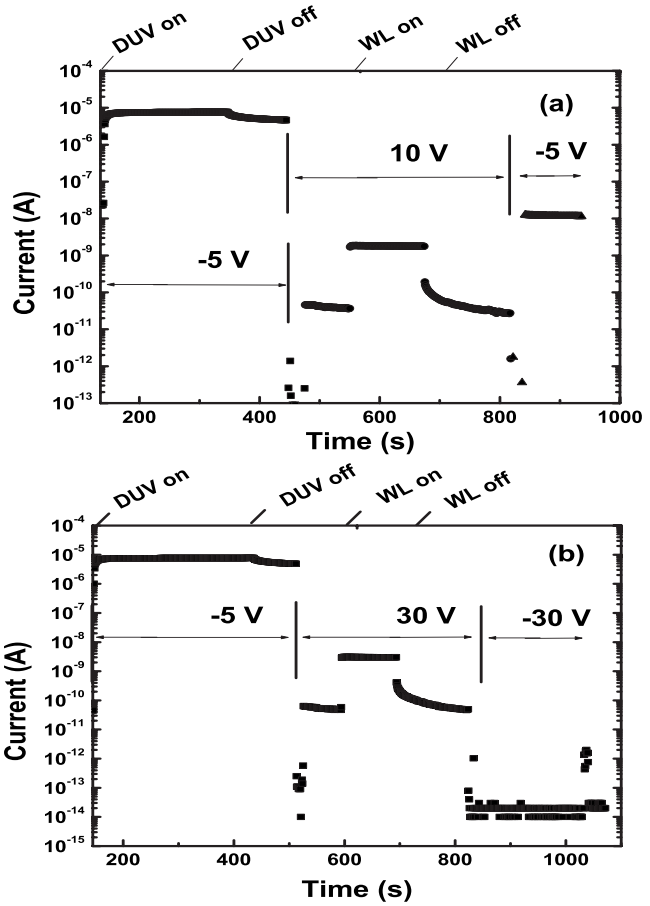

FIG. 9. Evolution of the PPPC with time upon the illumination of WL at (a) V_R=10 V and (b) V_R=30 V.

D. Absolute transient negative photocurrent

Figure 10(a) shows the time evolution of the photocurrent for SPD device A with DUV light illumination at zero bias after the optical quenching illustrated in Fig. 9(b). During the initial stage of illumination, an absolute transient negative photocurrent (TNPC), defined as a transient current flowing in the direction opposite to that of the external electric field, was observed. After a short period, the length of which depended on the DUV light intensity, the photocurrent became positive as normal. A TNPC was observed at low biases for both devices A and B.

To determine whether the TNPC depends on the device structure, we illuminated the MSM device made by using an unintentionally doped epilayer grown on a type Ib diamond substrate (device C) with WL. The device showed very low dark current ($<10^{-13}$ A) up to 30 V and almost no PPPC. The WL illumination was carried out at a large bias of 30 V, after which the device was kept in the dark at this bias for hundreds of seconds. Following this quenching process, the device was again illuminated with DUV light. An absolute TNPC appeared for both bias polarities as long as the bias was low enough. As shown in Fig. 10(b), a more distinct absolute TNPC was observed at a small positive bias of 2 mV. Therefore, the TNPC is independent of the device structure.

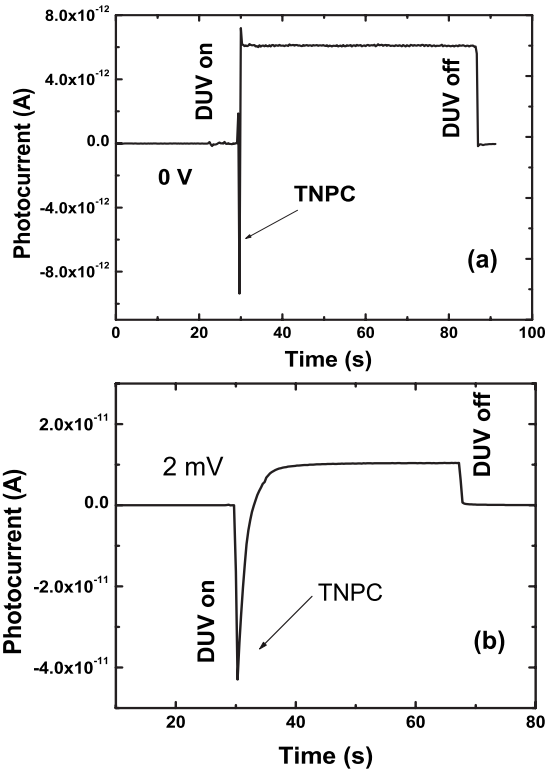

FIG. 10. Transient response upon the 220-nm light illumination after the optical quenching process as described in Fig. 9(b) for (a) SPD device A at 0 V and (b) MSM device C at 2 mV. An absolute TNPC appears at the initial excitation.

Similar quenching experiments were carried out for the MSM devices fabricated directly on a type Ib substrate (device D) and an unintentionally doped epilayer (device E) on a type IIa diamond substrate. The absolute TNPC was not observed for either device.

E. Optical quenching spectrum

The spectral dependence of the PPPC quenching for device A was examined immediately after DUV light illumination. The wavelength was varied from 630 to 210 nm, and the scanning direction was from long to short wavelengths with a step of 2 nm. The time interval, Δt, between two data points was 3, 10, 20, or 30 s with V_F=−5 V. The photocurrent decay in the dark is shown in a solid line within a similar period to ensure the reliability of the spectral quenching. As shown in Fig. 11, a decrease in the PPPC was observed at wavelengths (λ) ranging from 350 to 550 nm for Δt=3 s. The threshold wavelength of 550 nm shifted slightly to a longer wavelength as Δt was increased. On the short wavelength side, the current increased when the wavelength was smaller than 350 nm (3.5 eV), which agrees with our previous photocurrent spectrum.[11,19] Therefore, monochromatic light with λ from 350 to 500 nm can quench the PPPC effect. Quenching by any wavelength in this range with DUV light illumination is capable of bringing forward an absolute TNPC.

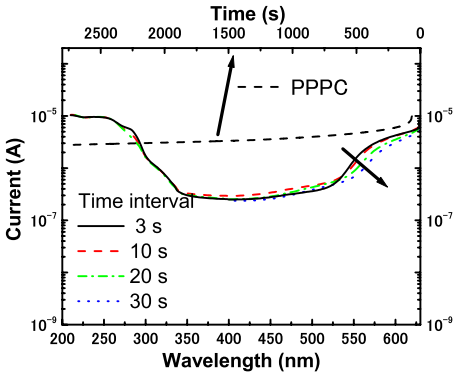

FIG. 11. (Color online).Quenching spectra of the PPPC at −5 V after DUV light illumination for different time intervals between two points.

IV. DISCUSSION

We first summarize our experimental results briefly. (a) The DUV photosensitivity and the PPPC were sensitive to the boron concentration. A larger boron concentration produced a larger DUV photosensitivity and a stronger PPPC. (b) A deep defect with a thermal activation energy of around 1.37 eV was found by the TSC measurement. The PPPC effect was quenched by photons with a threshold energy of around 2 eV. (c) The optical quenching of the PPPC effect depended on the applied bias polarity for the SPD devices. (d) An absolute TNPC appeared at low biases with DUV light illumination after quenching at high biases for both the SPD and MSM devices. The dependence of the PPPC and TNPC effects on the sample and device structure is summarized in Table II.

A. Mechanism of PPPC and gain

The SPD device structure revealed that the photocurrent at forward biases was dominated by holes, as can be seen from the rectified photocurrent-voltage dependence for *p*-type Schottky contacts. The increase in the photocurrent is a result of the increase in hole density Δp in the valence band. For *p*-type diamond SPD, the contact for holes is ohmic at large biases, but the electron flow from metal to diamond is blocked. When the forward bias is larger than the built-in voltage, the gain can be described as $G=1+\epsilon_h/\epsilon_e$ if there are no defects.[22] Given that electron mobility ϵ_e is larger than hole mobility ϵ_h,[24] the photocurrent gain at forward biases larger than the built-in voltage of the ideal SPD is principally no more than two. The appearance of a gain of more than 10^3 (Fig. 3) accompanied by PPPC implies the existence of a deep defect in the device.

TABLE II. Summary of PPPC and TNPC effects

Device	Sample	PPPC	TNPC
A	Boron-doped epilayer/Ib	Yes	Yes
B	Unintentionally doped epilayer/Ib	No	Yes
C	Unintentionally doped epilayer/Ib	No	Yes
D	Ib substrate	No	No
E	Unintentionally doped epilayer/IIa		No

We considered two origins for the carrier trapping, microscopic deep defect E_t located in the epilayer and macroscopic nitrogen defect E_N in the substrate, as illustrated in Fig. 12(a), which shows an equilibrium band diagram for the substrate/epilayer/WC junction. The SPD device structure and the contact nature for diamond ensure that the dominant TSC signal is due to holes, while the electron current is trivial due to the high barrier in the diamond/metal interface for electrons. The increase in the TSC current as the temperature (RT-470 K) increased means there was an increase in the free hole density in the epilayer, which can be simply understood by means of the detrapping of holes from an acceptor-like level in the lower half of the band gap. If the deep defect in the epilayer is donorlike and located in the upper half of the band gap, the thermal detrapping of electrons will lead to a reduction in the main signal rather than a peak in the TSC

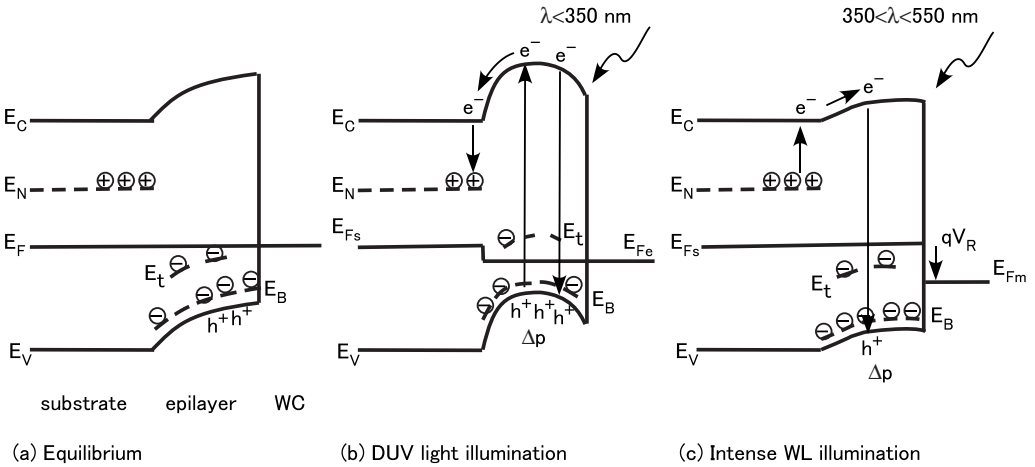

FIG. 12. Band diagrams showing (a) the depletion of holes in the epilayer and formation of positively charged nitrogen in the substrate at the equilibrium state, (b) trapping of electrons by the ionized nitrogen in the substrate during DUV light illumination, causing PPPC and gain at forward biases, and (c) optical quenching by sub-band-gap light at reverse biases through hole retrapping by the deep defect or the recombination between the electrons from the substrate nitrogen and the holes in the epilayer.

spectra due to the electron-hole recombination. Therefore, the defect E_t in the epilayer is more possibly acceptorlike, which may be related to boron. Increasing the boron content increases the density of this defect, which leads to a larger photocurrent. According to Lucovsky theory, photocurrent I_{PC} originating from a deep level E_i varies with photon energy $h\nu$ in accordance with $I_{PC} \propto (h\nu - E_{io})^{1.5}/(h\nu)^4$. By fitting Fig. 11 on the low-energy side, we obtained an optical threshold energy of $E_{io}=2$ eV. This value is considerably larger than the corresponding thermal energy of 1.37 eV, suggesting that this defect exhibits a large lattice relaxation. However, the second origin, the nitrogen in the substrate, contributes significantly to the PPPC and gain effects since they appeared only with UV light illumination. In this case, the homojunction between the epilayer and the substrate leads to the depletion of the epilayer holes, which forms positively charged nitrogen in the substrate near the interface [Fig. 12(a)]. Figure 12(b) shows a nonequilibrium band diagram for DUV light illumination, which explains the mechanism of increasing Δp. The charged nitrogen acts as a deep trap for electrons under DUV light illumination. The filling of the N^+ trap level mainly results from the photogenerated electrons in the conduction band. The increase in the boron concentration in the epilayer also increases the density of the positively charged nitrogen in the substrate, leading to a larger photocurrent gain. Due to the deep nature of nitrogen and to the potential barrier between the substrate and the epilayer, the photocurrent gain was always accompanied by strong PPPC for the boron-doped epilayer. In fact, the optical threshold for the quenching was similar to the energy for the photoionization of the nitrogen in type Ib diamond.[25] However, the thermal activation energy of 1.4–1.5 eV measured by either the TSC or PPPC decay experiments was smaller than that of nitrogen (1.7 eV), and the strong PPPC and gain effects depended strongly on the boron content. Therefore, we conclude that the PPPC and gain effects were due to both microscopic and macroscopic defects. Note that there is no evident dependence of the PPPC effect on the surface morphology of the diamond thin film. From the TSC curve in Fig. 4, we observed a rapid quenching at high temperatures (>530 K), which caused difficulty in determining the second peak energy.

During DUV light illumination, the nitrogen level in the substrate was mostly occupied by electrons, and the deep defect in the epilayer was mostly occupied by holes, supported by the TSC experiment. If the DUV intensity is strong, the excess carrier density is much larger than the trap density so the numbers of excess holes and electrons are nearly equal. For weak DUV light excitation, as was the case in the present experiments, the traps affect the photocurrent significantly. In the simple case where only positive-charged nitrogen plays a major role, the photocurrent gain in the steady state can be described by[26]

$$\Delta p/\Delta n = \tau_p/\tau_n = (1 + \mathrm{N_N}/n_{NF}), \tag{3}$$

where Δp and Δn are the excess hole and electron concentrations, respectively, τ_p and τ_n are the lifetimes of the excess holes and electrons, respectively, and n_{NF} is the carrier density when the Fermi level is set to the same as the deep level position. Calculation based on Eq. (3) revealed that the positive-charged nitrogen density, $\mathrm{N_N}$, was unreasonably low, supporting the complex trapping and detrapping process discussed above. An increase in the boron concentration increases both the E_t and E_N density, thus increasing the photocurrent gain and simultaneously the decay time. Control of the boron concentration is therefore very important in balancing the sensitivity and response speed. On the other hand, random local-potential fluctuation (RLPF) has also been proposed for the PPPC state in semiconductors.[27] However, we found that the PPPC effect was stronger at lower temperatures and that it was thermally quenched at higher temperatures. This is a typical feature of deep defects. Also, no obvious dependence of the PPPC effect on the DUV light intensity and the forward biases (larger than the built-in voltage) was observed. Therefore, RLPF is unlikely the main reason for the PPPC here.

B. Origin of PPPC quenching

The mechanism of the PPPC quenching is discussed using Fig. 12(c), which shows a band diagram illustrating the quenching process using WL illumination at reverse biases following DUV light illumination. When the illumination was done using sub-band-gap photons with energies in the range 2.2–3.5 eV, there was simultaneous capture of holes from the valance band by the deep defect related to boron and ionization or reionization of the nitrogen in the substrate. The former effect causes the current to return to the original state, which is the usual detrapping process.[28] The ionization of nitrogen generated free electrons [Fig. 12(c)], which depletes the free holes in the epilayer to a density lower than the initial dark value, causing negative photoconductivity.[22,29] The speeding up of the optical quenching process at high reverse biases is evidence that nitrogen originates from the substrate since high reverse biases lower the barrier for electrons between the substrate and the epilayer. Because the nitrogen in diamond is a deep defect, the negative photoconductivity is also persistent. If the boron concentration is sufficiently low, the device will be persistently insulating after the quenching process because the holes are completely depleted in the epilayer, which was observed experimentally [Fig. 9(b)]. The participation of the substrate nitrogen in the photoresponse was supported by the appearance of visible light response at higher reverse biases.[19] Due to the optical quenching, the DUV photocurrent for the device fabricated on the epilayer/Ib (100) diamond substrate decreased when a WL was illuminated simultaneously with the DUV light. The disappearance of PPPC with the WL light illumination confirms that nitrogen also plays a role in recombination. The PPPC quenching is a slow process since electrons (substrate) and holes (epilayer) are separated in space.

C. Mechanism of TNPC

An interesting question concerns the origin of the absolute TNPC, which differs from the traditional negative photoconductivity.[23,29] The absolute TNPC has been treated theoretically for bulk GaAs and InSb semiconductors, which

was in nanosecond scale due to the partial inversion of the photoexcited electron distribution in the transient regime.[30] It was regarded that the absolute TNPC was difficult to observe either in bulk or heterostructure semiconductors with stationary photoexcitation.[30] Nevertheless, we observed the absolute TNPC in a nearly second scale under a stationary condition. We excluded the effect of charge accumulation near the electrodes by observing the TNPC in a symmetrical MSM photoconductor. The absence of TNPC in devices D and E demonstrates that TNPC is due to an interaction between the epilayer and the substrate. After quenching the PPPC effect with WL illumination, free electrons generated in the epilayer with DUV light illumination diffuse to the substrate and fill in the ionized nitrogen. In the initial stage of DUV illumination, the predominant current arises from the electron flow from the epilayer to the substrate. As more electrons are generated, the ionized nitrogen level is neutralized, and the epilayer becomes conductive. Therefore, the absolute TNPC is the transient electron current from the electrodes to the substrate. In fact, TNPC can only be observed for low electric fields smaller than the built-in potential at the interface between the substrate and epilayer. In our case, for the unintentionally doped diamond epilayer, the maximal voltage for the observation of the TNPC effect was 5 V. Our observation of the absolute TNPC further supports that the nitrogen in the substrate quenches the PPPC.

To summarize briefly, the nitrogen in the substrate along with the boron in the epilayer tailor the overall photoresponse properties of a thin epilayer deposited on a type Ib diamond substrate: (i) the substrate nitrogen reduces the subband photoresponse in the visible light regime through optical quenching, (ii) the ionization of the neutral nitrogen speeds up the response time, and (iii) the trapping of electrons by the positively charge nitrogen in the substrate combined with the boron in the epilayer increases the DUV sensitivity. The formation of a homojunction between the substrate and epilayer means that even a thin homoepitaxial layer can improve the spectral response of a diamond photodetector significantly.

V. CONCLUSION

In conclusion, PPPC and photocurrent gain were observed on boron-doped homoepitaxial thin films grown on type Ib diamond substrates. The PPPC and gain effects were explained in terms of the boron-induced deep defect with a thermal activation energy of 1.37 eV and the spatially charged nitrogen in the substrate. Optical quenching experiments revealed a threshold at around 2 eV, indicating that the defect exhibited a large lattice relaxation. The ionization of the nitrogen in the substrate with WL illumination quenched the PPPC state by depleting the holes in the epilayer, causing the photodetector insulating. An absolute TNPC appeared with DUV light illumination after WL quenching due to electron filling of the charged nitrogen level.

ACKNOWLEDGMENTS

This work was partially supported by a Grant-in-Aid for Scientific Research from the Japanese Ministry of Education, Culture, Sports, Science and Technology (No. 188517).

*Meiyong.Liao@nims.go.jp

[1] S. Lany and A. Zunger, Phys. Rev. B **72**, 035215 (2005).
[2] E. P. De Poortere, Y. P. Shkolnikov, and M. Shayegan, Phys. Rev. B **67**, 153303 (2003).
[3] B. Potì, A. Passaseo, M. Lomascolo, R. Cingolani, and M. De Vittorio, Appl. Phys. Lett. **85**, 6083 (2004).
[4] C. E. Nebel, A. Waltenspiel, M. Stutzmann, M. Paul, and L. Schafer, Diamond Relat. Mater. **9**, 404 (2000).
[5] J. M. Marshall and A. S. Walters, Diamond Relat. Mater. **9**, 408 (2000).
[6] S. Salvatori, E. Pace, M. C. Rossi, and F. Galluzzi, Diamond Relat. Mater. **6**, 361 (1997).
[7] A. Balducci, M. Marinelli, E. Milani, M. E. Morgada, G. Prestopino, M. Scoccia, A. Tucciarone, and G. Verona-Rinati, Appl. Phys. Lett. **87**, 222101 (2005).
[8] M. Y. Liao, Y. Koide, and J. Alvarez, Appl. Phys. Lett. **87**, 022105 (2005).
[9] M. Nesladek, Semicond. Sci. Technol. **20**, R19 (2005).
[10] A. De Sio, J. Achard, A. Tallarie, R. S. Sussmann, A. T. Collins, F. Silva, and E. Pace, Appl. Phys. Lett. **86**, 213504 (2005).
[11] M. Y. Liao and Y. Koide, Appl. Phys. Lett. **89**, 113509 (2006).
[12] J. Walker, Rep. Prog. Phys. **42**, 1605 (1979).
[13] M. W. Geis, K. E. Krohn, J. M. Lawless, Jr., S. J. Deneault, M. F. Marchant, J. C. Twichell, T. M. Lyszczarz, J. E. Butler, D. D. Flechtner, and R. Wright, Appl. Phys. Lett. **84**, 4620 (2004).
[14] C. E. Nebel, E. Rohrer, and M. Stutzmann, J. Appl. Phys. **89**, 2237 (2001).
[15] P. Muret, E. Gheeraert, and A. Deneuville, Phys. Status Solidi A **174**, 129 (1999).
[16] K. Thonke, Semicond. Sci. Technol. **18**, S20 (2003).
[17] J. Ruan, K. Kobashi, and W. J. Choyke, Appl. Phys. Lett. **60**, 3138 (1992).
[18] S. C. Lawson, H. Kanda, T. Tsutsumi, and H. Kawarada, J. Appl. Phys. **77**, 1729 (1995).
[19] M. Y. Liao, J. Alvarez, and Y. Koide, Jpn. J. Appl. Phys., Part 1 **44**, 7832 (2005).
[20] J. Alvarez, J. P. Kleider, P. Bergonzo, D. Tromson, E. Snidero, and C. Mer, Diamond Relat. Mater. **12**, 546 (2003).
[21] S. M. Sze, *Physics of Semiconductor Devices*, 2nd ed. (Wiley, New York, 1981).
[22] R. H. Bube, *Photoelectronic Properties of Semiconductors* (Cambridge University Press, Cambridge, England, 1992).
[23] D. R. Hang, Y. F. Chen, F. F. Fang, and W. I. Wang, Phys. Rev. B **60**, 13318 (1999).
[24] J. Isberg, J. Hammersberg, E. Johansson, T. Wikstrom, D. J. Twitchen, A. J. Whitehead, S. E. Coe, and G. A. Scarsbrook, Science **297**, 1670 (2002).
[25] E. Rohrer, C. F. O. Graeff, R. Janssen, C. E. Nebel, M. Stutzmann, H. Güttler, and R. Zachai, Phys. Rev. B **54**, 7874 (1996).
[26] S. K. Zhang, W. B. Wang, I. Shatu, F. Yun, L. He, H. Markoç, X.

Zhou, M. Tamargo, and R. R. Aifano, Appl. Phys. Lett. **81**, 4862 (2002).

[27] J. Y. Lin, A. Dissanayake, and H. X. Jiang, Phys. Rev. B **46**, 3810 (1992).

[28] J. Alvarez, J. P. Kleider, P. Bergonzo, C. Mer, D. Tromson, A. Deneuville, and P. Muret, Diamond Relat. Mater. **11**, 635 (2002).

[29] A. L. Powell, C. C. Button, J. S. Roberts, P. I. Rockett, H. G. Grimmeiss, and H. Pettersson, Phys. Rev. Lett. **67**, 3010 (1991).

[30] O. E. Raichev and F. T. Vasko, Phys. Rev. B **73**, 075204 (2006), and references therein.